Proceedings of the 28th IEEE
EMBS Annual International Conference
New York City, USA, Aug 30-Sept 3, 2006

Quantification of Carotid Atherosclerotic Plaque Components using Feature Space Analysis and Magnetic Resonance Imaging

Christof Karmonik, Pamela Basto, and Joel D. Morrisett

Abstract—**Atherosclerosis is one of the main causes of cardiovascular disease, accounting for more than one third of all deaths in the United States, there is a growing need to develop non-invasive techniques to assess the severity of atherosclerotic plaque burden. Recent research has suggested that not the size of the atherosclerotic plaque but rather its composition is indicative for plaque rupture as the underlying event of stroke and acute coronary syndrome. With its excellent soft-tissue contrast, magnetic resonance imaging (MRI) is a favored modality for examining plaque composition. In an ex-vivo study, aimed to show the feasibility of quantifying the components of carotid atherosclerotic plaques in-vivo, we acquired multi-contrast MRI images of 13 freshly excised endarterectomy tissues with commercially available MRI sequences and a human surface coil. Feature space analysis (FSA) was utilized in four representative tissues to determine the total relative abundance of calcific, lipidic, fibrotic, thrombotic and normal components as well as in consecutive 2 mm sections across the carotid bifurcation in each tissue. Excellent qualitative agreement between the FSA results and the results obtained from histological methods was observed. This study demonstrates the feasibility of combining MRI with FSA to quantify carotid atherosclerotic plaques in-vivo.**

I. Introduction

The prevalence for cardiovascular disease (CVD) in the United States in 2003 amounted to 34.2 % of the total population. This corresponds to health care costs of $403.1 billion for 2006. Of all the deaths suffered from CVD, 53.5 % are attributed to coronary heart disease and 17 % to Stroke with atherosclerosis as its underlying cause [1].

While the mechanisms of atherogenesis remain uncertain, the response-to-injury theory is widely accepted. Circulating monocytes infiltrate the injured vessel wall resulting in subendothelial accumulation of cholesterol-engorged macrophages ('foam cells') leading to so-called fatty-streak lesions. While not clinically significant, these fatty-streak lesions are precursors of more advanced lesions containing a lipid-rich necrotic core and smooth muscle cells (SMC). These SMC together with the extracelluar matrix typically form a thin fibrous cap enclosing the necrotic core. Complexity of plaque composition can increase further, involving calcification, ulceration at the luminal surface, and hemorrhaging from small blood vessels penetrating the lesion.

Although atherosclerotic plaques are able to grow and thereby gradually occlude the vessel, the more serious clinical event is the acute occlusion due to the formation of thrombus leading to myocardial infarction (coronary arteries) or stroke (carotid arteries). Thrombus formation is usually associated with rupture or erosion of the fibrous cap covering the lesion. Recent results indicate that it is not the size of the plaque but rather its composition that is an indicator of the severity of the disease and risk for rupture [2]. A noninvasive method for characterizing plaque composition would therefore be highly beneficial for assessing clinical risk.

Among all non-invasive medical imaging modalities, magnetic resonance imaging (MRI) is one of the best suited to examine the composition of atherosclerotic plaque tissue because of its excellent soft-tissue contrast originating from the local molecular environment of the proton spins. Multi-contrast approaches in MRI have been utilized both in vivo and ex vivo to identify features in atherosclerotic plaque tissue. Lipidic, calcific, fibrotic and thrombotic tissue components have been observed to exhibit different MRI image intensity using various MRI acquisition techniques [3] – [8].

It would be highly advantageous to combine the information contained in MRI images acquired with different parameters into one single image for visualization and quantitative analysis of the plaque composition.

Feature space analysis (FSA) or cluster analysis is a well established technique that partitions a set of objects into relatively homogeneous subsets based on inter-object similarities [9].

In an *ex vivo* study of excised coronary atherosclerotic plaque tissue, multi-contrast MRI images (proton-density weighted (PDW), T2-weighted (T2W), intermediate weighting) were segmented using FSA [10]. An *ex vivo* MRI study at 9.4 T has described quantifying mineralization content in atherosclerotic tissue using k-means clustering and employing PDW, T2W, T1-weighted (T1W) and diffusion weighted MRI. [11]. The classification based on k-means cluster analysis of 9.4T MRI images (T1W, T2W and PDW) from coronary atherosclerotic plaque tissue showed very good agreement with histopathology images for all AHA classification plaque types [12].

Manuscript received April 3, 2006. This work was supported in part by the National Institutes of Health under Grants RO1-HL63090 and T32-HL02812.

C. Karmonik is a Research Scientist with The Methodist Hospital, Houston, TX 77030 USA (phone: 713-441-1583; fax: 713-790-6474; ckarmonik@ tmh..tmc.edu.)

P. Basto was a Summer Medical And Research Training (SMART) student with Baylor College of Medicine, Houston, TX 77030 USA.

J. D. Morrisett is Professor of Medicine and Biochemistry at Baylor College of Medicine, Houston, TX 77030 USA (morriset@bcm.tmc.edu).

The aim of the present study was to test the feasibility of MRI combined with FSA for the development of a non-invasive clinical technique to characterize carotid atherosclerotic plaque composition *in vivo*. For that purpose, we acquired *ex-vivo* MRI images of excised carotid endarterectomy tissues using conditions that mimic clinical *in vivo* conditions. A k-means clustering algorithm was then used to segment the calcific, lipidic, thrombotic, fibrotic and normal tissue components. The results obtained with this algorithm were compared to histological results obtained from thin slices of selected sections of the atherosclerotic tissues. Sectional and total composition of the investigated atherosclerotic plaque tissues were calculated.

II. Methods

A. MRI Image Acquisition

Thirteen freshly excised carotid endarterectomy tissues typically 30-50 mm long and 5 – 15 mm in diameter were obtained 1 – 3 hrs after resection. At each imaging session, four tissues were placed in 15 ml plastic culture tubes filled with TBS and placed in a water-filled cylindrical sample holder with approximately the same diameter as the human neck. Images were acquired using a 6 cm phased array coil (Pathway Medical Technologies, Inc.) developed for human carotid plaque imaging on a GE 1.5 T Excite full-body MRI scanner. Consecutive axial PDW (TE=15 ms, TR=2400 ms, echo train length=8) , T1W (TE=15 ms, TR=600 ms, echo train length=3) and T2W (TE=94 ms, TR=4000 ms, echo train length=18) images were acquired (slice thickness 2 mm, matrix 512x384 zero-filled to 512x512, FOV 100 mm x 100 mm) using a fast-spin echo sequence providing 8 – 31 slices depending on the size of tissue with an in-plane resolution of 0.195 mm. Four tissues were selected for analysis with FSA and histology.

B. Feature Space Analysis

Images were transferred to an off-line PC workstation equipped with the NIH ImageJ image post-processing software [13]. Images were enlarged by a factor of two using bilinear interpolation and image stacks for each tissue were created. A low-frequency bandpass filter based on a Fourier technique was used to correct the images for in-plane intensity inhomogeneities originating from the inhomogeneous surface coil sensitivity profile (Fig. 1). The through-plane image signal intensity was corrected as well, as determine d from the average signal intensity of the surrounding water in a user-selected region of interest placed near the culture tube containing the tissue. The correction of intensity inhomogeneities is necessary to ensure that the same tissue components will have similar image intensity values across the image stack. This is an essential prerequisite for application of feature space analysis.

The feature space considered in our analysis is the three-dimensional space spanned by the three gray scale image intensities of the PDW, T1W and T2W images so that the feature space coordinates of an image pixel are its image intensity values in the PDW, T1W and T2W images. The distance between two feature space points is given by their

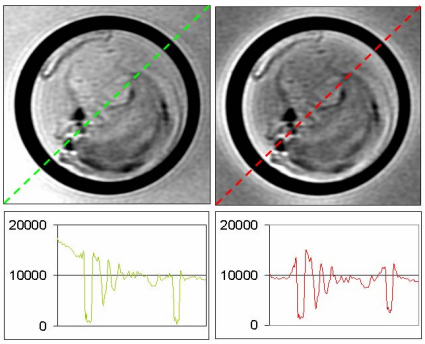

Fig. 1. Illustration of the in-plane image inhomogeneity correction. Top left: Uncorrected image, top right: corrected image. Bottom left: intensity profile along the dotted line in the image on top. Bottom right: intensity profile along the dotted line in the image on top. Image intensities of the water in the lower left and upper right corners in the corrected image are similar compared to the higher intensity in the lower left corner in the uncorrected image.

Euclidian distance calculated with these coordinates. A k-

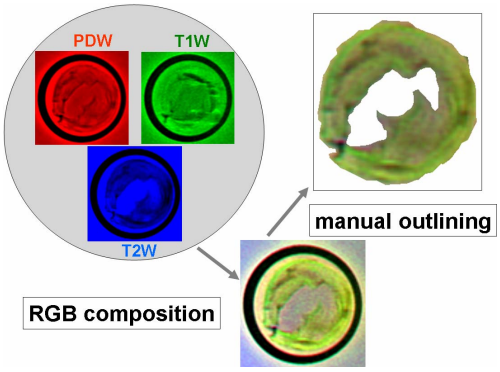

Fig. 2. From the PDW, T1W and T2W images, an RGB color composite was created as illustrated here for one image. The plaque tissue was then manually outlined to create the input images for the k-means cluster algorithm.

means clustering algorithm was used to find the point clusters in the feature space. The algorithm starts by randomly creating clusters from the input points. The algorithm then enters an iteration loop during which the assignment of the points to the clusters is changed until the sum of the distances of the cluster centers between two iteration steps is smaller than a convergence threshold value provided by the user. In each iteration step, the closest cluster center for each point is determined and each point is then re-assigned to its closest cluster center followed by a recalculation of the centers for each cluster. A software plugin for ImageJ was utilized to perform this k-means

cluster analysis [14].

For that purpose, PDW, T1W and T2W images were merged to a color RGB composite image with the PDW image as the red image component, the T1W image the green image component and the T2W image as the blue image component. For each slice, the plaque tissue was manually outlined and the image intensity values outside the so defined tissue boundaries were set to zero (Fig. 2).

Corresponding to the tissue components (calcific, fibrotic, thrombotic, lipidic and normal) that we intended to quantify, six clusters were allowed (providing one cluster for the background). The convergence threshold was chosen as 0.0001. For each tissue, relative abundance for each 2 mm segment along the carotid vessel axis and the total volumetric average values over all segments for these components were calculated.

C. Histology

After imaging, the tissues were cut into 5mm segments proceeding from the bifurcation into the common, external, and internal carotids. These segments were then imbedded in OCT and 5-10 µm thin sections were cut from each end of each segment, then mounted, stained with Masson-trichrome (TRI), van Giessen (VVG), or Oil Red O (ORO) reagents, then photographed using an Veritas LCM system (Arcturus).

III. Results

A. Feature Space Analysis

Fig. 3 shows selected RGB composite images of tissue #1 together with the segmented images obtained with the feature space analysis.

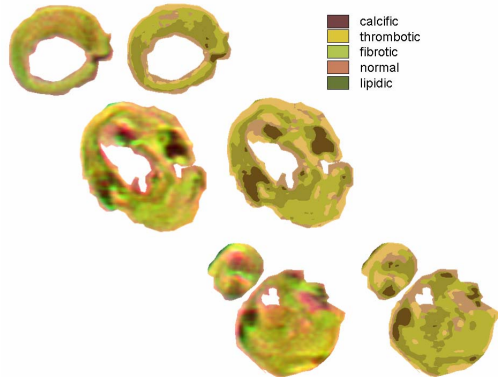

Fig. 3. Results of the k-means algorithm illustrated on selected images for one tissue. Images on top are from the part of the tissue located in the common carotid artery; images in the center are from near the carotid bifurcation; and images from the bottom are from the part of the tissue superior to the carotid bifurcation located in the external (left) and internal (right) carotid artery.

Fig. 4 illustrates the segmentation results in feature space and demonstrates the spatial distribution of each tissue component for tissue #1.

B. Histology

Fig. 5 shows the comparison of the FSA results with selected histology sections from the four tissues. For better visualization, the FSA images were rotated to better match the histology images.

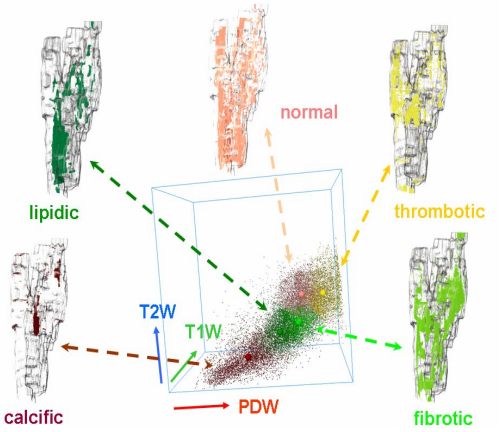

Fig. 4. FSA cluster analysis results for tissue #1 in feature space (center, blue outline). Centroids of clusters are marked by colored spheres. The dashed lines show the correspondence between the feature space clusters and the spatial distribution of the tissue components visualized. The tissue boundaries are indicated by the gray outline.

C. Compositional Analysis

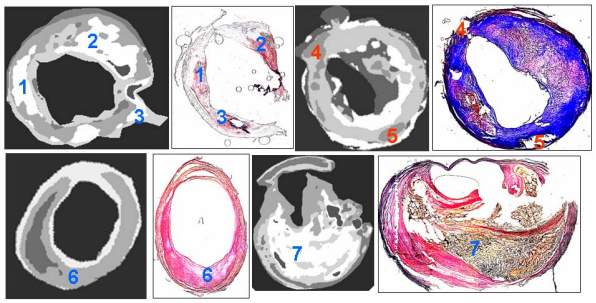

Fig. 5. Comparison of FSA results with histology results. Upper left: lipid region identified with ORO (red) match white areas in FSA image (regions 1,2,3). Upper right: calcific regions characterized by voids in a TRI section are identified in the FSA image (regions 4,5). Lower left: Large fibrotic region in the FSA image and the VVG section (region 6). Lower right: thrombotic tissue in the FSA image and the corresponding VVG section (region 7).

The position resolved relative abundance curves for the four tissues are presented in Fig. 6 and table 1 shows the total relative composition values.

IV. Discussion

FSA techniques are used in a variety of disciplines and many variations of cluster algorithms exist. In the present study, we chose the k-means cluster algorithm as it is one of the simplest unsupervised learning algorithms that will always terminate [15]. It does not require the user to provide cluster-specific input parameters nor is there a need to teach the algorithm by having the operator to select regions in the images representative of the clusters to be quantified. It is known that the k-means cluster algorithm is very sensitive to the starting positions of the initial centroids.. The stability of

the k-means algorithm was therefore assessed by varying the

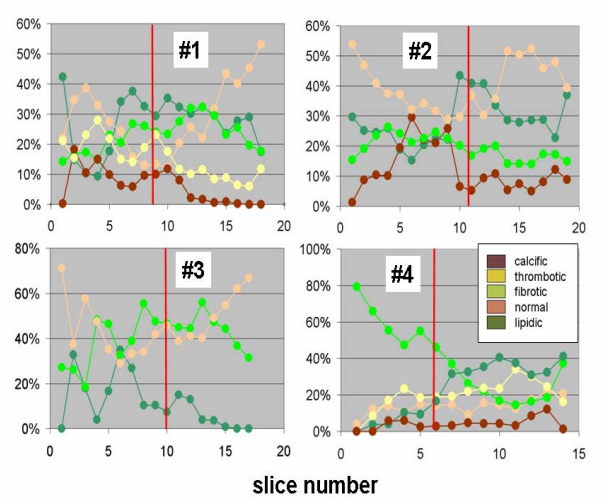

Fig. 6. Position-resolved relative abundance curves. Slices located in the common carotid are on the right and the red line marks the location of the carotid bifurcation.

operator-provided convergence threshold by an order of magnitude in the range from 1 to 0.00001. For each threshold value, the k-means analysis was repeated 5 times, each time with randomly determined initial positions of the centroid clusters. The standard deviation of the total number of pixels for each tissue component was then calculated as a measure for the reproducibility of the segmentation results For the values of a convergence threshold less than 0.1, the standard deviations in the number of points for each cluster was less than 0.07 %; for a value of 0.1, the average standard variation was 0.45 %; and for a value of 1, the average standard variation was 2.7 %. These results demonstrate good reproducibility of the algorithm and further show that the results are relatively independent of the convergence threshold if this threshold is less than 0.1

Comparison of the FSA images with results obtained by histologic methods is excellent considering that the slice thickness of the MRI images (2 mm) is several orders of magnitudes larger than the thickness of the histologic sections (<20 μm). Because of partial volume effects, the signal measured over the slice thickness of an MRI image is an average signal and does not necessarily reflect the exact composition of a histologic section from this slice.

In conclusion, this study demonstrates that cluster analysis can be utilized to quantify the major components of carotid atherosclerotic plaque tissue in a configuration very similar to clinical in-vivo imaging conditions and suggests cluster analysis combined with MRI may be successfully used to study atherosclerotic plaque composition *in vivo*.

ACKNOWLEDGMENT

The authors acknowledge the contributions of Iou Chan, Cathy Higgins, and Kasey Vickers to this work (TBTGA).

TABLE I
TOTAL RELATIVE COMPOSTION VALUES (%)

Tissue	#1	#2	#3	#4
calcifc	6	12	0	4
thrombotic	15	0	0	20
fibrotic	23	20	41	39
normal	29	40	47	14
lipidic	27	28	12	23

REFERENCES

[1] T. Thom, N. Haase, W. Rosamond, V.J. Howard, J. Rumsfeld, T. Manolio *et al*. Heart Disease and Stroke Statistics – 2006 Update. Circulation, 113(6):e85-e151, 2006.

[2] R. Virmani, F.D. Kolodgie, A.P. Burke, A. Farb, S.M. Schwartz. Arterioscler Thromb Vasc Biol 20:1262-1275, 2000.

[3] Z.A. Fayad and V. Fuster. Characterization of Atherosclerotic Plaques by Magnetic Resonance Imaging. AnnN Y Acad Sci. 902:173-86, 2000.

[4] C. Yuan, L.M. Mitsumori, M.S. Ferguson, N.L. Polissar, D. Echelard, G. Ortiz, R. Small, J.W. Davies, W.S. Kerwin, T.S. Hatsukami. In Vivo Accuracy of Multispectral Magnetic Resonance Imaging for Identifying Lipid-Rich Cores and Intraplaque Hemorrhage in Advanced Human Carotid Plaque. Circulation, 104:2051-2056, 2001.

[5] X.Q. Zhao, C. Yan, T.s. Hatsukami, E.H. Frechette, X.J. Kang, K.R. Maravilla, B.G. Brown. Effects of Prolonged Intensive Lipid-Lowering Therapy on the Characteristics of Carotid Atherosclerotic Plaques in Vivo by MRI. A Case-Control Study. Arterioscler Thromb Vase Biol. 2 1:1623-1629, 2001.

[6] T.S. Hatsukami, r. Ross, N.L. Polissar, C. Yuan. Visualization of fibrous cap thickness and rupture in human atherosclerotic carotid plaque in vivo with high- resolution magnetic resonance imaging. Circulation. 1 02(9):959-64, 2000.

[7] C. Yuan, L.M. Misumori, K.W. Beach, K.R. Maravilla. Carotid Atherosclerotic Plaque: Noninvasive MR Characterization and Identification of Vulnerable Lesions. Radiology 221:285-299, 2001.

[8] J.M. Serfaty, L. Chaabane, A. Tabib, J.M. Callier, A. Briguet, P.C. Douek. Atherosclerotic plaques: classification and characterization with T2-weighted high- spatial-resolution MR imaging-- an in vitro study. Radiology. 2001 May;219(2):403-10, 2001.

[9] S. K. Kachigan. Multivariate Statistical Analysis, Radius Press New York 261-270, 1991.

[10] J. Zheng, I. El Naqa, F.E. Rowold, T.K. Pilgram, P.K. Woodard, J.E. Saffitz, D. Tang. Quantitative assessment of coronary artery plaque vulnerability by high-resolution magnetic resonance imaging and computational biomechanics: A pilot study ex vivo. Magn Reson Med., 54(6):1360-8, 2005

[11] R.L. Wolf, S.L. Wehrli, A.M. Popescu, J.H. Woo, H.K. Song, A.C. Wright, *et al*. Mineral volume and morphology in carotid plaque specimens using high-resolution MRI and CT. Arterioscler Thromb Vasc Biol. 25(8):1729-35, 2005.

[12] V.V. Itskovich, D.D. Samber, V. Mani, J.G. Aguinaldo, J.T. Fallon, C.Y. Tang, V. Fuster, Z. A. Fayad. Quantification of human atherosclerotic plaques using spatially enhanced cluster analysis of multicontrast-weighted magnetic resonance images. Magn Reson Med.;52(3):515-23, 2004.

[13] W.S. Rasband, ImageJ, National Institutes of Health (NIH), http://rsb.info.nih.gov/ij/, 1997-2005.

[14] S. Jarek, ImageJ plugin, http://ij-plugins.sourceforge.net/plugins/clustering/index.html

[15] J. B. MacQueen. "Some Methods for classification and Analysis of Multivariate Observations, Proceedings of 5-th Berkeley Symposium on Mathematical Statistics and Probability", Berkeley, University of California Press, 1:281-297, 1967.